Supporting Online Material for

Noncanonical TGFβ Signaling Contributes to Aortic Aneurysm Progression in Marfan Syndrome Mice

Tammy M. Holm, Jennifer P. Habashi, Jefferson J. Doyle, Djahida Bedja, YiChun Chen, Christel van Erp, Mark Lindsay, David Kim, Florian Schoenhoff, Ronald D. Cohn, Bart L. Loeys, Craig J. Thomas, Samarjit Patnaik, Juan J. Marugan, Daniel P. Judge, Harry C. Dietz

*To whom correspondence should be addressed. E-mail: hdietz@jhmi.edu

Published 15 April 2011, *Science* **332** 358 (2011)
DOI: 10.1126/science.1192149

This PDF file includes

Supporting Online Material

Materials and Methods

Mice

All mice were cared for under strict compliance with the Animal Care and Use Committee of the Johns Hopkins University School of Medicine. The *Smad4* haploinsufficient mice were a generous gift from Dr. Chuxia Deng (NIH/NIDDK, Bethesda). The *Fbn1*$^{C1039G/+}$ line was maintained on a C57BL/6 background, allowing for valid comparisons. In order to further accommodate the potential for temporal- or background-specific variation in genetic or pharmacological manipulation experiments, all comparisons were made between contemporary littermates. Mice were checked daily for death and all mice found dead were immediately necropsied to assess for evidence of aortic dissection. Mice were killed with an inhalation overdose of halothane (Sigma-Aldrich, St. Louis). Mice underwent immediate laparotomy, descending abdominal aortic transection, and PBS (pH 7.4) infusion through the left ventricle to flush out the blood. For Western blot analysis, the proximal ascending aorta (root to right brachiocephalic trunk) was removed, flash frozen in liquid nitrogen and stored at –80^{o}C. Following PBS infusion, mice analyzed for aortic histology had latex injected under low pressure into the left ventricular apex until it was visible in the descending abdominal aorta. The mice were then fixed for 24 hours in 10% buffered formalin, after which the heart and aorta were removed and stored in 70% ethanol.

Medication

Mouse monoclonal TGFβNAb (1d11; R&D Systems, Minneapolis) was reconstituted in PBS and administered via intraperitoneal injection 3 times a week at a dose of 5mg/kg. Treatment was initiated at 1 month of age and continued for 2 months. IgG (Zymed Laboratories Inc, San Francisco) was reconstituted in PBS, and administered at a dose of 10mg/kg as a control. SP600125 (Sigma-Aldrich, St. Louis) was reconstituted in 10% DMSO dissolved in PBS, and administered twice daily by intraperitoneal injection, at a dose of 30 mg/kg. Treatment was initiated at 1 month of age and continued for 2 months. 10% DMSO dissolved in PBS was administered as a control. RDEA119 was reconstituted in 10% 2-hydroxypropyl-beta-cyclodextrin (Sigma-Aldrich, St. Louis) dissolved in PBS, and administered twice daily by oral gavage at a dose of 25 mg/kg. Treatment was initiated at 2 months of age and continued for 2 months. 10% 2-hydroxypropyl-beta-cyclodextrin dissolved in PBS was administered as a control. Fasudil was dissolved in drinking water, and administered at a dose of 1 mg/kg body weight per day. Treatment was initiated at 2 months of age and continued for 4 months. Drinking water was administered as a control.

Echocardiography

Nair hair removal cream was used on all mice the day prior to echocardiography. All echocardiograms were performed on awake, unsedated mice using the Visualsonics Vevo 660 V1.3.6 imaging system and a 30 MHz transducer. The aorta was imaged using a parasternal long axis view. Three separate measurements of the maximal internal systolic dimension at the sinus of Valsalva and proximal ascending aorta were made, and a mean

was calculated. All imaging and measurements were performed by a cardiologist who was blinded to genotype and treatment arm. In the TGFβNAb and SP600125 trials, mice were imaged at 1 month (baseline) and 3 months of age, after which they were killed. In the RDEA119 trial, mice were imaged at 2 months (baseline) and 4 months of age, after which they were killed. In the fasudil trial, mice were imaged at 2 months (baseline) and 6 months of age, after which they were killed. *Smad4* haploinsufficient mice were imaged at 1 month, and then every 2 months thereafter, until death or sacrifice.

Western Blot Analysis

Protein was extracted using the reagents and protocol from a Total Protein Extraction Kit, in conjunction with a Protein Phosphatase Inhibitor Cocktail (Millipore, MA). Aortas were homogenized using a pellet pestle motor (Kimble-Kontes, NJ) as per the extraction kit protocol. Homogenates were dissolved in sample buffer, run on a NuPAGE Bis-Tris Gel (Invitrogen, CA), and transferred to nitrocellulose membranes using the iBlot transfer system (Invitrogen, CA). Membranes were washed in PBS and blocked for 1 hour at room temperature with 5% instant non-fat dry milk, dissolved in PBS containing 1% Tween-20 (Sigma, MO) (PBS-T). Equal protein loading of samples was determined by a protein assay (BioRad, CA) and confirmed by probing with antibodies against β-Actin or GAPDH (Sigma, MO). Membranes were probed overnight at 4^{o}C with primary antibodies from Santa Cruz, CA (pERK1/2, pJNK1/2) and Cell Signaling, CA (pSmad2, Smad2, ERK1/2, JNK1, pp38, p38, pMEK1, MEK1, pERK5, ERK5, ROCK1, pLIMK1, Smad4, pSmad2, PAI-1, pSmad3 and Smad3) dissolved in PBS-T containing 5% milk. Blots were then washed in PBS-T, and probed for 1 hour at room temperature with HRP-conjugated secondary antibodies (GE Healthcare, UK) dissolved in PBS-T containing 5% milk. Blots were then washed in PBS-T, developed using SuperSignalWest HRP substrate (Pierce Scientific, IL), exposed using BioMax Scientific Imaging Film (Sigma, MO) and quantified using ImageJ analysis software (NIH, MD).

Histological Analysis

Latex-infused ascending aortas were transected just above the level of the aortic valve, and 2- to 3-mm transverse segments were mounted in 4% agar. These were then paraffin embedded and sectioned. Sections underwent Verhoeff-van Giesen (VVG) staining and were imaged at 40x magnification, using a Nikon Eclipse E400 microscope. Four representative VVG images of each mouse aorta were assessed by 3 blinded observers and graded on a scale of 1 (indicating no elastic fiber breaks) to 5 (indicating extensive elastic fiber fragmentation). An aortic wall architecture score was calculated by averaging the results of the 3 blinded observers. Sections also underwent trichrome staining to assess the degree of collagen deposition in the aortas of these mice.

Statistical Analysis

All values are expressed as means $\pm$ 2 standard errors of the mean (2SEM). Student *t* tests were used to evaluate significance between groups, with a p-value of $\leq$0.05 considered statistically significant.

Supporting Online Material (SOM) Text

To evaluate the effect of RhoA/ROCK pathway inhibition on aortic root growth, WT and *Fbn1*$^{C1039G/+}$ mice were treated with fasudil at a dose (1mg/kg) previously shown to rescue ROCK-mediated phenotypes in mice (*S1*).

Since ERK1/2 is a pro-proliferative intracellular mediator, the reduction in aortic root growth achieved in *Fbn1*$^{C1039G/+}$ mice could simply have been a result of decreased somatic growth of the whole animal. We therefore weighed all mice at the end of the 2 month trial, and found that RDEA119 therapy did not significantly affect the weight of either WT or *Fbn1*$^{C1039G/+}$ mice (Fig.S6). This supports the conclusion that the reduction in growth achieved by RDEA119 in *Fbn1*$^{C1039G/+}$ mice was specific to the aorta, and was not simply a manifestation of reduced somatic growth of the animal.

SP600125 was administered using a dosing regimen (30mg/kg twice-daily by intraperitoneal injection) that was previously shown to cause clinically-relevant JNK antagonism in other murine models of disease (*S3*).

The exacerbation of aortic disease in *Smad4* haploinsufficient MFS mice raises the question of whether Smad signaling is protective in MFS mice. For example, loss of Smad-driven collagen production in *S4+/-:Fbn1*$^{C1039G/+}$ mice could lead to aortic wall weakness and consequent rupture. Such a model is hard to support given the observation that both TGFβNAb and losartan achieve significant aortic protection in *Fbn1*$^{C1039G/+}$ mice, despite their documented suppression of canonical TGFβ signaling. To further address this issue, we performed trichrome staining on the aortas of WT, *S4+/-*, *Fbn1*$^{C1039G/+}$ and *S4+/-:Fbn1*$^{C1039G/+}$ mice (Fig.S7). This shows a relative increase in collagen deposition in *Fbn1*$^{C1039G/+}$ and *S4+/-:Fbn1*$^{C1039G/+}$ mice, compared to WT and *S4+/-* littermates. It also shows that there is comparable aortic collagen content in *Fbn1*$^{C1039G/+}$ and *S4+/-:Fbn1*$^{C1039G/+}$ mice, eliminating collagen deficiency as the mechanistic basis for aortic dissection and premature death in *S4+/-:Fbn1*$^{C1039G/+}$ mice.

Blockade of Smad activation (e.g. by Smad7 overexpression or by Smad2/3 siRNA) is an alternative approach to addressing the role of Smad signaling in MFS mice. However, these approaches would likely have resulted in increased inflammation, increased TGFβ ligand expression, and/or the activation of alternate pathways in our mice. Furthermore, Smad7 overexpressing mice die by 10 days of life (*S4*), and in-vivo use of siRNA-based methods are extremely challenging. We therefore concluded that *Smad4* haploinsufficiency was most likely the best way to reach meaningful conclusions. The fact that the clinical phenotype of *Fbn1*$^{C1039G/+}$ and *S4+/-:Fbn1*$^{C1039G/+}$ mice showed invariant correlation with ERK and/or JNK signaling, but not Smad signaling, supports our conclusion that ERK and JNK are prominent drivers of aortic disease in MFS mice.

Our data provide added incentive to explore new agents that inhibit ERK and/or JNK signaling. The long-term use of MAPK antagonists could theoretically have deleterious side effects. It is worth noting that both *erk1*-/- and *erk1*-/- *erk2*+/- mice survive, with no overt phenotypic defect. The mechanistic basis of the embryonic lethality seen in *erk2*-/- mice is not known, but it suggests that ERK2 is of critical importance during development. By contrast, inhibition of ERK1 and ERK2 activation by RDEA119 is well tolerated post-natally in mice, as well as in humans (*S5*), and shows significant therapeutic benefit in our study. This appears to be analogous to TGFβ, where deficiency states are not tolerated during development, but are better tolerated and show

phenotypic benefit postnatally. Finally, given losartan's profound inhibition of ERK activation, it is notable that losartan has been used for decades in patients without any apparent long-term deleterious consequences.

Supplemental Figures and Figure Legends

Fig. S1

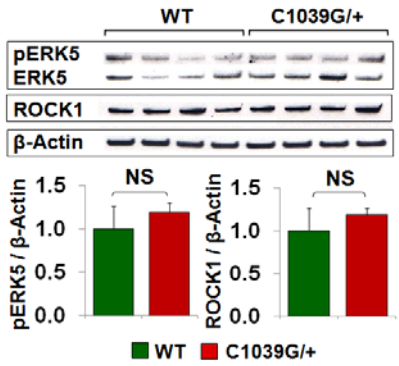

Fig. S1. Western blot analysis of the proximal ascending aorta of WT and *Fbn1*$^{C1039G/+}$ mice. Note that there is no difference in either pERK5 or ROCK1 when normalized to β-Actin. Values are Mean ± 2SEM. NS non-significant.

Fig. S2

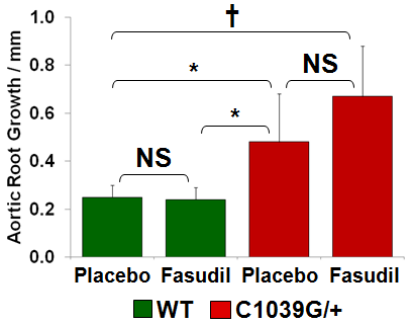

Fig. S2. Aortic root growth over 4 months, measured by echocardiography, in placebo-treated WT (n=10) and *Fbn1*$^{C1039G/+}$ (n=8) mice, and fasudil-treated WT (n=5) and *Fbn1*$^{C1039G/+}$ (n=6) mice. Note the lack of rescue of aortic root growth in fasudil-treated *Fbn1*$^{C1039G/+}$ mice. Absolute final aortic root diameter: placebo-treated WT (1.71±0.06), placebo-treated *Fbn1*$^{C1039G/+}$ (2.19±0.18), fasudil-treated WT (1.73±0.05), fasudil-treated *Fbn1*$^{C1039G/+}$ (2.40±0.16). Values are Mean ± 2SEM. ∗ $p<0.05$, † $p<0.001$, NS non-significant.

Fig. S3

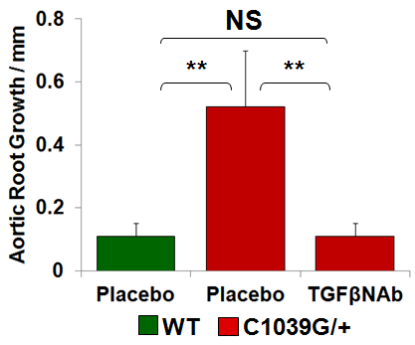

Fig. S3. Aortic root growth over 2 months, measured by echocardiography, in placebo-treated WT (n=6) and *Fbn1*$^{C1039G/+}$ (n=5) mice, and TGFβNAb-treated *Fbn1*$^{C1039G/+}$ mice (n=4). Note the full rescue of aortic root growth in TGFβNAb-treated *Fbn1*$^{C1039G/+}$ mice. Final absolute aortic root diameter: placebo-treated WT (1.66±0.06), placebo-treated *Fbn1*$^{C1039G/+}$ (2.19±0.18), TGFβNAb-treated *Fbn1*$^{C1039G/+}$ (1.96±0.6). Values are Mean ± 2SEM. ∗∗ $p<0.01$, NS non-significant.

Fig. S4

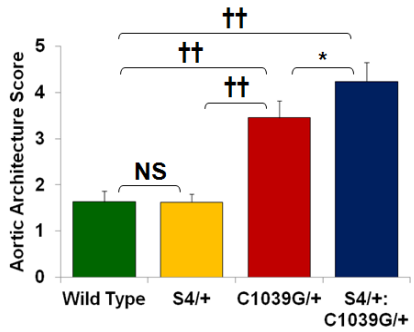

Fig. S4. Aortic architecture score in WT (n=12), *S4*+/- (n=10), *Fbn1*$^{C1039G/+}$ (n=8) and *S4*+/-*:Fbn1*$^{C1039G/+}$ (n=10) mice. While *Fbn1*$^{C1039G/+}$ mice are worse than WT mice, there is an exacerbation in *S4*+/-*:Fbn1*$^{C1039G/+}$ animals. Values are Mean ± 2SEM. ∗ $p<0.05$, †† $p<0.0001$, NS non-significant.

Fig. S5

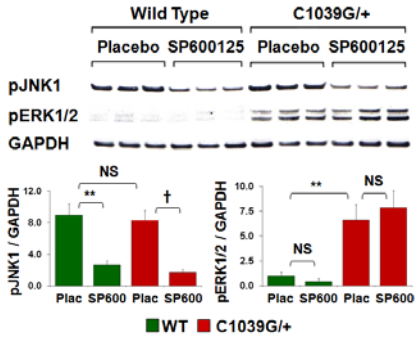

Fig. S5. Western blot analysis of the proximal ascending aorta of WT and *Fbn1*$^{C1039G/+}$ mice after 2 weeks of therapy with SP600125 or placebo. While there is a significant reduction in JNK1 activation in SP600125-treated animals to levels below baseline, there is no change in ERK1/2 activation. All normalized to GAPDH. Values are Mean ± 2SEM. ∗∗ $p<0.01$, † $p<0.001$, NS non-significant.

Fig. S6

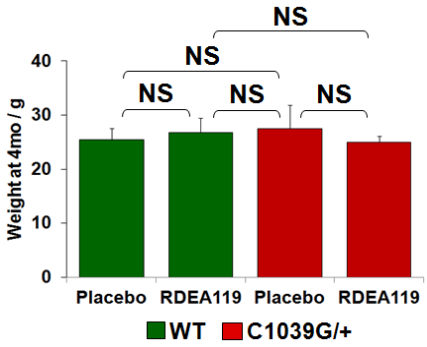

Fig. S6. Weight of placebo-treated WT (n=5) and *Fbn1*$^{C1039G/+}$ (n=6) mice, and RDEA119-treated WT (n=3) and *Fbn1*$^{C1039G/+}$ (n=7) mice, at the end of the 2 month trial. Note that RDEA119 treatment does not significantly affect somatic growth in either WT or *Fbn1*$^{C1039G/+}$ mice. Values are Mean ± 2SEM. NS non-significant.

Fig. S7

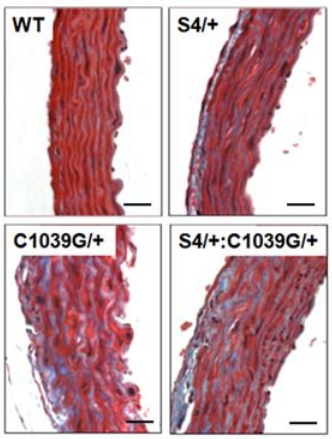

Fig. S7. Trichrome staining of representative proximal ascending aortic sections, showing increased collagen deposition in *Fbn1*$^{C1039G/+}$ and *S4*+/-*:Fbn1*$^{C1039G/+}$ mice, compared to WT littermates. Note the collagen content is comparable in *Fbn1*$^{C1039G/+}$ and *S4*+/-*:Fbn1*$^{C1039G/+}$ mice.

Supplemental References

S1. Y. X. Wang *et al*., *Circulation*. **111**, 2219 (2005).
S2. B. L. Bennett *et al*., *Proc. Natl. Acad. Sci. USA.* **98**, 13681 (2001).
S3. P. R. Eynott *et al*., *B. J. Pharmacol*. **140**, 1373 (2003).
S4. W. He *et al.*, *EMBO J*. **21**, 2580 (2002).
S5. www.ardeabio.com.